JOURNAL OF GUIDANCE, CONTROL, AND DYNAMICS
Vol. 28, No. 2, March–April 2005

Evaluation and Comparison of Relative Motion Theories

K. T. Alfriend* and H. Yan†
Texas A&M University, College Station, Texas 77843

A modeling error index is introduced for evaluating and comparing the accuracy of various theories of the relative motion of satellites to determine the effect of modeling errors on the various theories. The derived index does not require linearization of the equations of motion, and so nonlinear theories can also be evaluated. The index can be thought of as proportional to the percentage error; consequently, the smaller the index, the more accurate the theory. The results show that not including the reference orbit eccentricity and differential gravitational perturbations has a major effect on the accuracy of the theory, and the nonlinear effects are much smaller except for very large relative motion orbits. The two key parameters in the evaluation are the eccentricity of the reference orbit and the relative motion orbit size. The theories compared are Hill's equations, a small eccentricity state transition matrix, a non-J_2 state transition matrix, the Gim–Alfriend state transition matrix, the unit sphere approach, and the Yan–Alfriend nonlinear method. The numerical results show the sequence of the index from high to low should be Hill's equation, non-J_2, small eccentricity, Gim–Alfriend state transition matrix index, with the unit sphere approach and the Yan–Alfriend nonlinear method having the lowest index and equivalent performance.

Nomenclature

a	=	semimajor axis
e	=	eccentricity
i	=	inclination
J_2	=	equatorial bulge gravitational potential coefficient
(L, G, H, l, g, h)	=	Delaunay variables
(M, E, f)	=	mean, eccentric, and true anomalies
n	=	mean motion
(q_1, q_2)	=	nonsingular variables ($e\cos\omega$, $e\sin\omega$)
R_e	=	Earth radius
$\Re$	=	Hamiltonian
r	=	orbit radius
t	=	time
(x, y, z)	=	radial, in-track, and out-of-plane relative position
α_0	=	relative motion orbit phase angle
(λ, θ)	=	mean and true arguments of latitude
μ	=	gravitational coefficient
ν	=	modeling error index
ρ	=	measure of relative motion orbit size
Φ	=	state transition matrix
Ω	=	right ascension
ω	=	argument of perigee

Introduction

THIS paper is concerned with the comparing theories of the relative motion of two satellites. The reference satellite will be referred to as the chief, and the other satellite will be the deputy.

The analysis of the relative motion of satellites began with the paper by Clohessy and Wiltshire (CW),[1] who in 1960 derived the equations of motion for one satellite relative to another when the chief satellite is in a circular orbit about a spherical Earth. They also assumed that the separation distance between the satellites was small compared to the orbit radius so that the equations of motion could be linearized. These are sometimes called Hill's equations because Hill used the same approach in his research on the moon.[2] Because Clohessy and Wiltshire were concerned with rendezvous, long-term accuracy of the solution was not a major concern. Lawden[3] and Tschauner and Hempel[4] obtained independently the solution to the linearized equations of motion when the reference satellite is in an elliptical orbit. There were other efforts[5,6] in the 1960s to expand the solutions to include the first-order nonlinear terms and the first-order eccentricity effects. Although there are a few papers, e.g., Ref. 7, on the use of these equations over the next 30 years, it was not until the formation-flying concept began to be considered that we saw renewed interest. With the desire for accurate long-term prediction, there was a need for more accurate solutions to the relative motion problem. Gim and Alfriend[8] used a new approach to obtain the state transition matrix for the linearized equations for the reference satellite in an elliptic orbit that included the first-order absolute and differential J_2 effects. Inalhan and How[9] investigated the effects of neglecting the reference orbit eccentricity when establishing the relative motion initial conditions. References 10–12 were attempts to obtain corrections to the initial conditions to account for the nonlinear terms for the periodic relative motion orbits. They did not consider the general solution to the nonlinear equations. Alfriend and coworkers[13,14] developed a new approach to the nonlinear problem using differential orbital elements.

The complexity of the relative motion theories increases as the accuracy improves. Thus, an important question is which theory is needed for a given problem or what needs to be included in the reference orbit model. Because the accuracy is a function of the initial conditions, a methodology is needed for comparing the accuracy of the theories for a class of problems. Such a methodology was developed by Junkins et al.[15] for comparing linear theories. In Ref. 15 a nonlinear index was introduced for comparing the accuracy of various linearized solutions for the propagation of a debris cloud resulting from a collision or breakup. The analysis showed that when using the linearized equations of motion the most accurate solution is obtained by using differential orbital elements. Recently, Junkins[16] in his tutorial on nonlinearity of orbit and attitude dynamics discussed problems on how to measure nonlinearity and used the nonlinearity index to evaluate several coordinate choices.

In this paper we compare various theories for relative motion orbits and provide results that should aid mission designers in deciding which effects need to be included in the reference orbit model for their particular formation. The effects considered are the chief satellite eccentricity, absolute and differential J_2, and nonlinearity. Differential drag can have a significant effect but is not considered

Received 24 November 2003; revision received 12 May 2004; accepted for publication 13 May 2004.

*TEES Distinguished Research Chair Professor of Aerospace Engineering; alfriend@aero.tamu.edu. Fellow AIAA.

†Graduate Student, Department of Aerospace Engineering; hyan@tamu.edu.

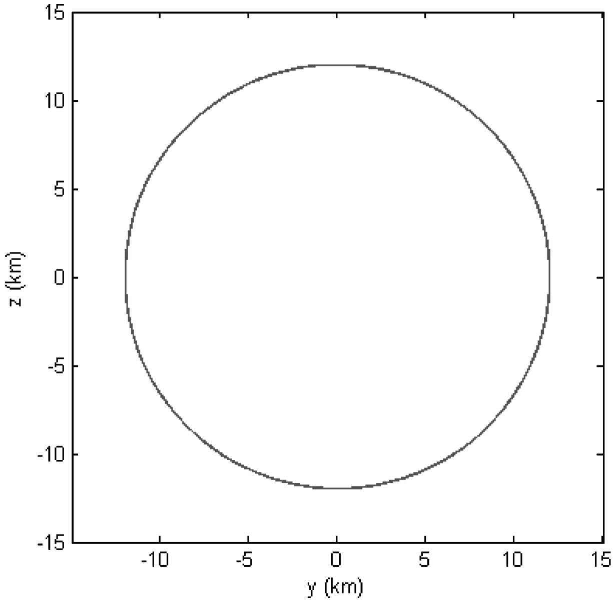

Fig. 1 Projected circular orbit, as defined in the along-track/cross-track plane.

because it is difficult to quantify because it is a function of altitude and differential ballistic coefficient. To evaluate the effect of the preceding factors, we selected theories that represent a sufficient cross section of modeling the just-mentioned effects. The theories selected for comparison are the CW solution,[1] the Gim–Alfriend[8] state transition matrix, a small eccentricity state transition matrix, a non-J_2 state transition matrix derived from the Gim–Alfriend state transition matrix that is equivalent to that derived by Lawden[3] and Tschauner and Hempel,[4] a unit sphere approach proposed by Vadali,[17] and Sengupta et al.,[18] and the Alfriend–Yan nonlinear theory.[13,14] There are numerous other theories in the literature, but inclusion of all of them is not reasonable, and the results provided here should be sufficient for assessing the accuracy of those theories. A new modeling error index derived from the Junkins nonlinearity index is used to compare the theories. The Junkins index cannot be used because it is restricted to linear theories. Comparisons are performed for a spherical Earth and an oblate Earth. When $J_2 = 0$, the Gim–Alfriend theory is numerically identical to the Lawden[3] and Tschauner–Hempel[4] theories, and so their accuracy is captured in these comparisons. The relative motion orbit selected for comparison is the projected circular orbit[19] (PCO) or its equivalent when the reference orbit is not circular. As shown in Fig. 1, the projected circular orbit is the relative motion orbit whose projection on the local horizontal plane is a circle. This relative motion orbit was selected because the evaluation of the relative motion theories should include some out-of-plane motion. The two key parameters in the evaluation are the eccentricity of the reference orbit and the relative motion orbit size, e.g., the projected circular orbit radius.

Modeling Error Index

Consider the nonlinear differential equations with the initial conditions:

$$\boldsymbol{x} = \boldsymbol{f}(t, \boldsymbol{x}), \qquad \boldsymbol{x}(t_0) = \boldsymbol{x}_0 \tag{1}$$

In Refs. 15 and 16 the nonlinearity index used was

$$\nu(t, t_0) = \sup_{i=1\ldots N} \frac{\|\Phi_1(t, t_0) - \bar{\Phi}(t, t_0)\|}{\|\bar{\Phi}(t, t_0)\|} \tag{2}$$

where $\bar{\Phi}(t, t_0)$ is the state transition matrix that is obtained from Eq. (1) with the expected initial conditions $\bar{\boldsymbol{x}}(t_0)$. $\Phi(t, t_0)$ is a state transition matrix that is obtained from Eq. (1) from a set of initial conditions that represents the worst-case relative to the expected initial conditions. For example, if the problem is a breakup or explosion the worst-case initial conditions would be the points on the surface of the 3σ ellipsoid of the relative velocity created by the breakup. In Ref. 15 this index was used to compare the accuracy of three linear theories for a circular reference orbit, the CW equations, the linear theory using polar coordinates, and one obtained from differential orbital elements. The objective was to determine which theory best captured the nonlinear effects. The comparison showed that differential orbital elements were the most accurate.

The nonlinearity index should evaluate modeling error, not just nonlinearity. Because the index in Eq. (2) cannot be used with a nonlinear theory, a new index is needed. In addition, our objective is to compare the accuracy of the theories for specific types of orbits. For comparison in this paper, the projected circular orbit (or its equivalent for a noncircular reference orbit) is used as the baseline orbit. Let $\bar{\boldsymbol{x}}_i(t)$ be the solution for the initial condition $\bar{\boldsymbol{x}}_i(t_0)$ at the corresponding points, and let $\boldsymbol{x}_i(t)$ be the solutions for the proposed models. These need not be linearized solutions. It is important that the states be in dimensionless variables or a weighting matrix used. Let $\boldsymbol{W}$ be a weighting matrix that nondimensionalizes $\boldsymbol{y}$, that is,

$$\boldsymbol{y} = \boldsymbol{W}\boldsymbol{x} \tag{3}$$

We now propose the following modeling error index:

$$\nu(t) = \max_{i=1\ldots N} |\nu_i| \tag{4a}$$

$$\nu_i = \frac{\bar{\boldsymbol{y}}_i^T \bar{\boldsymbol{y}}_i}{\boldsymbol{y}_i^T \boldsymbol{y}_i} - 1 \tag{4b}$$

Note that if there is only one state and we let $y_i = \bar{y}(1+\gamma)$, then the index becomes $\upsilon = 2|\gamma|$. Therefore, the index is proportional to the percentage error.

Reference Orbits

We use differential orbital elements to set up a reference relative motion orbit or projected circular orbit. Then we take many points on the orbit as initial conditions and propagate them to obtain the model error index as a function of time.

We begin with the Hamiltonian of the reference satellite's motion expressed in terms of mean orbital elements. Assume $\varepsilon = -J_2$. In normalized Delaunay variables with $\mu = 1$, $R_e = 1$, the averaged Hamiltonian to the first order is[20]

$$\Re = -1/2L^2 + \varepsilon(1/4L^6)(L/G)^3[-1 + 3(H^2/G^2)] \tag{5}$$

where $L = \sqrt{(\mu a)}$, $G = L\sqrt{(1-e^2)} = L\eta$, $H = G\cos i$, and $\varepsilon = -J_2$.

Mean elements are used because the angle rates are constant, which means the constraints to minimize or prevent drift between the satellites are a function of only the momenta (L, G, H) or (a, e, i). If the starting point is the Hamiltonian in osculating space, the constraints are also a function of the angles, and the relative motion orbit is more difficult to design. We use the mean argument of latitude $\lambda = l + \omega$, where l is the mean anomaly. The angle rates in the mean space are

$$\dot{\lambda} = \frac{\partial\Re}{\partial L} + \frac{\partial\Re}{\partial G} = \frac{3\varepsilon}{4L^7}\left(\frac{L}{G}\right)^3\left[\left(1 - 3\frac{H^2}{G^2}\right) + \left(\frac{L}{G}\right)\left(1 - 5\frac{H^2}{G^2}\right)\right] \tag{6}$$

$$\dot{\omega} = \frac{\partial\Re}{\partial G} = \frac{3\varepsilon}{4L^7}\left(\frac{L}{G}\right)^4\left(1 - 5\frac{H^2}{G^2}\right) \tag{7}$$

$$\dot{\Omega} = \frac{\partial\Re}{\partial H} = \frac{3\varepsilon}{2L^7}\left(\frac{L}{G}\right)^4\frac{H}{G} \tag{8}$$

Because relative orbit design is more direct in terms of (e, i) instead of (G, H), we will use these as the momenta variables. The angle rates become

$$\dot{\lambda} = 1/L^3 + (3\varepsilon/4L^7\eta^4)[(1+\eta) - (5+3\eta)\cos^2 i] \quad (9)$$

$$\dot{\omega} = (3\varepsilon/4L^7\eta^4)(1 - 5\cos^2 i) \quad (10)$$

$$\dot{\Omega} = (3\varepsilon/4L^7\eta^4)\cos i \quad (11)$$

The period matching condition for the relative motion at first order is[8]

$$\delta\dot{\lambda} + \delta\dot{\Omega}\cos i = 0 \quad (12)$$

In this paper we have selected the projected circular relative motion orbit (PCO) for comparing the relative motion theories. In a chief-centered local-vertical/local-horizontal (LVLH) frame, the PCO can be described by[19]

$$x = 0.5\rho\sin(\theta + \alpha_0) \quad (13)$$

$$y = \rho\cos(\theta + \alpha_0) \quad (14)$$

$$z = \rho\sin(\theta + \alpha_0) \quad (15)$$

where θ is the latitude angle of the chief satellite. We want to express Eqs. (13–15) in terms of the orbital elements in the mean space. To avoid the singularity at small eccentricity, they should be a set of nonsingular orbital elements. We have selected the following:

$$\boldsymbol{e} = [a, \lambda, i, q_1, q_2, \Omega], \qquad q_1 = e\cos\omega, \qquad q_2 = e\sin\omega \quad (16)$$

The differential orbital elements are determined from the selected relative motion orbit. They are[21]

$$\delta\lambda = -\delta\Omega\cos i \quad (17)$$

$$\delta i = \frac{\rho\cos\alpha_0}{a} \quad (18)$$

$$\delta q_1 = -\frac{\rho\sin\alpha_0}{2a} \quad (19)$$

$$\delta q_2 = -\frac{\rho\cos\alpha_0}{2a} \quad (20)$$

$$\delta\Omega = -\frac{\rho\sin\alpha_0}{a\sin i} \quad (21)$$

From Eq. (12) the difference in the semimajor axis is

$$\delta a = -0.5J_2 a(R_e/a)^2[(3\eta+4)/\eta^4] \times \left\{(1 - 3\cos^2 i)[(q_1\delta q_1 + q_2\delta q_2)/\eta^2] + \sin 2i\,\delta i\right\} \quad (22)$$

By choosing values of α_0 between 0 and 360 deg, we obtain a distribution of the initial conditions. Starting with these initial conditions, we evaluate the modeling error index of the approximate methods.

Approximate Methods for Relative Motion

Hill's Equations

Hill's equations are established in the LVLH frame by making the assumptions of a circular chief orbit, spherical Earth, linearizing the differential gravity accelerations, and neglecting all other perturbations. Hill's equations are

$$\ddot{x} - 2n\dot{y} - 3n^2x = 0 \quad (23)$$

$$\ddot{y} + 2n\dot{x} = 0 \quad (24)$$

$$\ddot{z} + n^2 z = 0 \quad (25)$$

where x, y, and z are the LVLH Cartesian coordinates, and $\dot{x}$, $\dot{y}$, and $\dot{z}$ are the relative velocity components in the frame. Hill's equations have analytical solutions,[22] so that they can easily be used to approximate the relative motion.

Gim–Alfriend State Transition Matrix

Because Hill's equations have considerable errors and are insufficient for long-term prediction, Gim and Alfriend[8] developed an accurate state transition matrix for the perturbed noncircular reference orbit using a geometrical method. Realizing the deputy relative motion is a result of small changes in the orbital elements of the chief, they used differential orbital elements and then transformed into the LVLH coordinates. The linear approximation using the differential orbital elements is more accurate than that using the Cartesian or curvilinear coordinates as shown in Refs. 15 and 16. Moreover, using the differential orbital elements automatically includes the reference or chief orbit eccentricity, which is not included in Hill's equations. Notice this method does not require the solution of differential equations. The state transition matrix is

$$\boldsymbol{X}(t) = \{\boldsymbol{A}(t) + \alpha\boldsymbol{B}(t)\}\delta\boldsymbol{e} \quad (26)$$

or

$$\boldsymbol{X}(t) = \{\boldsymbol{A}(t) + \alpha\boldsymbol{B}(t)\}\boldsymbol{D}(t)\bar{\phi}_e(t, t_0)\boldsymbol{D}^{-1}(t_0)\{\boldsymbol{A}(t_0) + \alpha\boldsymbol{B}(t_0)\}^{-1}\boldsymbol{X}(t_0) \quad (27)$$

where $\boldsymbol{X} = [x\ \dot{x}\ y\ \dot{y}\ z\ \dot{z}]$ is the relative motion coordinate vector $\alpha = 3J_2R_e^2$, the matrix $\boldsymbol{B}(t)$ contains only the terms perturbed by J_2, $\bar{\phi}_e(t)$ is the state transition matrix for the relative mean elements, and $\boldsymbol{D}(t)$ is the Jacobian of the mean to osculating element transformation.

Small-Eccentricity State Transition Matrix

The Gim–Alfriend state transition matrix is valid for any eccentricity, but it is complex with many terms. A less complex version for small eccentricity can be derived by retaining $\mathcal{O}(e)$ terms for the non-J_2 portion and only $\mathcal{O}(e^0)$ for the J_2 portion. See the Appendix for the state transition matrix.

Non-J_2 State Transition Matrix

The matrix is obtained from Eq. (27) by setting $J_2 = 0$. Its accuracy is numerically identical to those in the Lawden[3] and Tschauner–Hempel[4] theories. Therefore, its evaluation is equally applicable to evaluating either Lawden or Tschauner–Hempel.

Unit Sphere Approach

In the unit sphere approach,[17,18] the relative motion problem is studied by projecting the motion of the two satellites onto a unit sphere. This is achieved by normalizing the position vector of each satellite with respect to its radius. This process allows one to study the relative motion using spherical trigonometry so that a kinematically exact description is obtained for the relative positions in terms of the differential orbital elements, without recourse to linearization. To obtain time-explicit expressions, the method uses Kepler's equation or eccentricity expansions to obtain the radial distance and argument of latitude. Taking time derivatives for the relative positions, we get analytical expressions for the relative velocities with the help of Gauss' equations.

The relative position on the unit sphere is given by

$$\begin{Bmatrix} \Delta x \\ \Delta y \\ \Delta z \end{Bmatrix} = \left[C_c C_D^T - I\right]\begin{Bmatrix} 1 \\ 0 \\ 0 \end{Bmatrix} \quad (28)$$

where Δx, Δy, and Δz are, respectively, the radial, along-track, and cross-track relative positions on the unit sphere and C is the direction cosine matrix that transforms a vector in the Earth-centered inertial (ECI) frame to one in the LVLH frame. The subscripts C and D stand for quantities pertaining to the chief and deputy, respectively. Δ

represents quantities pertaining to the deputy minus those pertaining to the chief. This results in analytical expressions for the so-called subsatellite points that are functions of the angles only. The matrix C is given by

$$C = \begin{pmatrix} \cos\theta\cos\Omega - \sin\theta\cos i\sin\Omega & \cos\theta\sin\Omega + \sin\theta\cos i\cos\Omega & \sin\theta\sin i \\ -\sin\theta\cos\Omega - \cos\theta\cos i\sin\Omega & -\sin\theta\sin\Omega + \cos\theta\cos i\cos\Omega & \cos\theta\sin i \\ \sin i\sin\Omega & -\sin i\cos\Omega & \cos i \end{pmatrix} \quad (29)$$

The actual relative positions between the two satellites are

$$x = r_D(1+\Delta x) - r_c, \qquad y = r_D\Delta y, \qquad z = r_D\Delta z \quad (30)$$

Taking time derivatives, we have

$$\dot{x} = \dot{r}_D(1+\Delta x) + r_D\Delta\dot{x} - \dot{r}_C, \qquad \dot{y} = \dot{r}_D\Delta y + r_D\Delta\dot{y}$$

$$\dot{z} = \dot{r}_D\Delta z + r_D\Delta\dot{z} \quad (31)$$

where r_C and r_D are the radii of the chief and deputy, respectively. The expressions for Δx, Δy, Δz, $\Delta\dot{x}$, $\Delta\dot{y}$, $\Delta\dot{z}$, can be found in Ref. 21.

Using Kepler's equation,

$$M_j = E_j - e_j\sin(E_j), \qquad j = C, D \quad (32)$$

$$\dot{E}_j = \frac{\dot{M}_j + \dot{e}_j\sin(E_j)}{1 - e_j\cos(E_j)} \quad (33)$$

$$r_j = a_j[1 - e_j\cos(E_j)] \quad (34)$$

$$\dot{r}_j = \dot{a}_j[1 - e_j\cos(E_j)] + a[\dot{E}_j e_j\sin(E_j) - \dot{e}_j\cos(E_j)] \quad (35)$$

The other time derivatives such as $\dot{a}$, $\dot{e}$, $\dot{i}$, $\dot{f}$ can be obtained from Gauss's variational equations.[21]

Yan–Alfriend Nonlinear Method

The geometrical method by Alfriend and Gim is just a transformation from a nonlinear algebra into a linear one. It results in not only a daunting task, but the linearization creates a nonlinear error. However, because the linearization is performed in orbital element space the error is smaller than if the equations of motion were solved in Cartesian space.[15] The Yan–Alfriend method is also performed in orbital element space. It extends the earlier work of Schaub and Alfriend[23] in that the Taylor-series expansion of the deputy mean orbital elements about the chief is carried to second order. The matching condition to suppress the in-track drift is then determined, and the time history of the differential mean elements determined. Because the expansion is carried to second order, the J_2^2 terms are included. This constitutes a very simple method for a long-term prediction for nonlinear relative motion, that is, we predict mean orbital elements at the given time for the noncircular reference orbit including nonlinear J_2 effects and then transform them into the LVLH coordinates. Details are provided in Refs. 13, 14, and 21.

Numerical Results

Let us define several test cases for which we can evaluate the modeling error index for each approximate method. Let the mean orbital elements of the chief take on the following values:

$$a = 8000\text{ km}, \qquad i = 50\text{ deg}$$

$$\Omega = 0\text{ deg}, \qquad \omega = 0\text{ deg}, \qquad M_0 = 0\text{ deg}$$

$$e = 1e-4, 5e-4, 0.001, 0.005, 0.01, 0.05, 0.1$$

We use these elements and Eqs. (17–22) to establish the PCO for a circular chief orbit. When the chief orbit is not circular, they establish a relative motion orbit that is close to a PCO. Because the period matching condition is used, there is very little in-track drift. The radius ρ of the PCO is chosen as 0.16, 0.80, 1.6, 4, 8, 12, 16, 40, 80, 120, and 160 km. See Fig. 1 for the PCO when $e = 0.001$ and $\rho = 12$ km. The objective is to evaluate the index given by Eq. (4) for each of the approximate methods, varying the eccentricity of the chief orbit and the PCO radius. For each case (specific value of e and ρ) 100 equally spaced values of the phase angle α_0 between 0 and 360 deg are used. In Eq. (3), $\boldsymbol{x} = [x\ \ \dot{x}\ \ y\ \ \dot{y}\ \ z\ \ \dot{z}]$, and select $\boldsymbol{W}$ in terms of the Earth-value units so that $\boldsymbol{y}$ has canonical units. We used for $\boldsymbol{W}$

$$\boldsymbol{W} = \mathrm{diag}(1/R_e, 1/R_e, 1/R_e, 1/R_e n_0, 1/R_e n_0, 1/R_e n_0)$$

$$n_0 = \sqrt{\mu / R_e^3} \quad (36)$$

Using Eq. (4), index ν_i is evaluated for each of the initial phase angles, and the index value is obtained. Notice $\bar{y}_i$ in Eq. (4) is obtained by numerically integrating the equations of motion of both the chief and deputy in the ECI reference frame with a J_2 gravity field, and then transforming the position and velocity vectors from the ECI frame to the chief frame.

Figures 2–9 show the index comparisons varying with the eccentricity of the chief orbit and the PCO radius.

Figures 2–9 show the modeling error index at the end of one day for the six theories: Hill's equation, small eccentricity, non-J_2, Gim–Alfriend, unit sphere approach, and Yan–Alfriend nonlinear method. Figures 2–5 show the effect of the index as a function of the size of the orbit for various eccentricities. Figures 6–9 show the effect of the index as a function of eccentricity for various size orbits. The index provides a method for comparing the accuracy of various theories. As shown earlier in the one-dimensional case, the index is representative of twice the percentage error. In the n-dimensional case the acceptable value for an index can only be determined by what size errors are acceptable for the mission. Many factors such as minimum time between thruster firings, allowable error growth rate, and allowable error impact the decision of the specific model to be used. The method presented here only provides a guideline for determining which theory or what dynamic effects need to be included in the model, for a specific problem. Also, keep in mind that the index represents the maximum error over all of the initial conditions for the PCO. There are initial conditions for which the

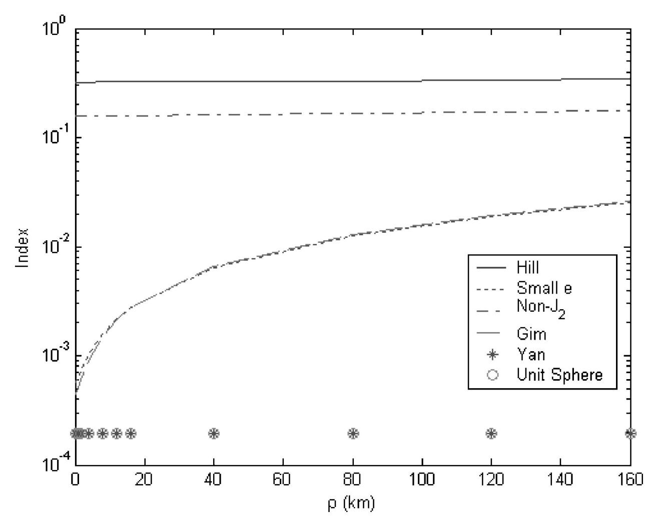

Fig. 2 Index comparison for $e = 0.0001$.

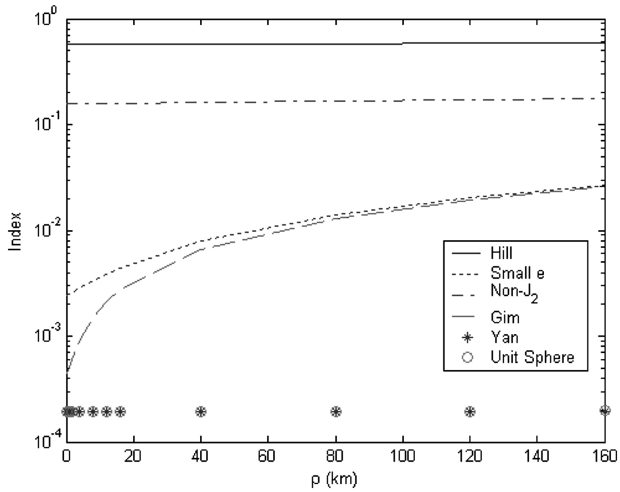

Fig. 3 Index comparison for $e = 0.001$.

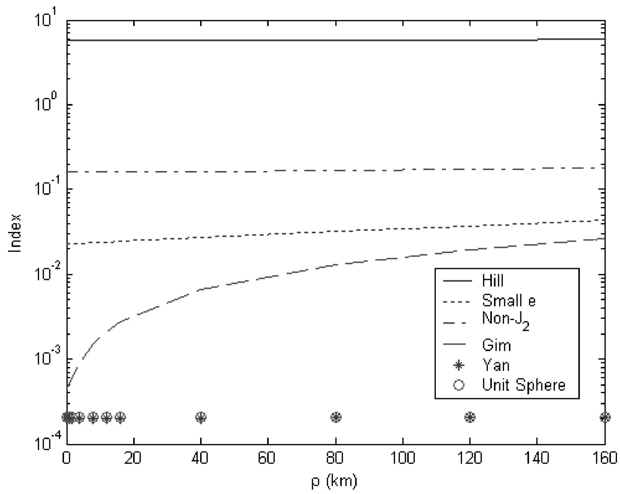

Fig. 4 Index comparison for $e = 0.01$.

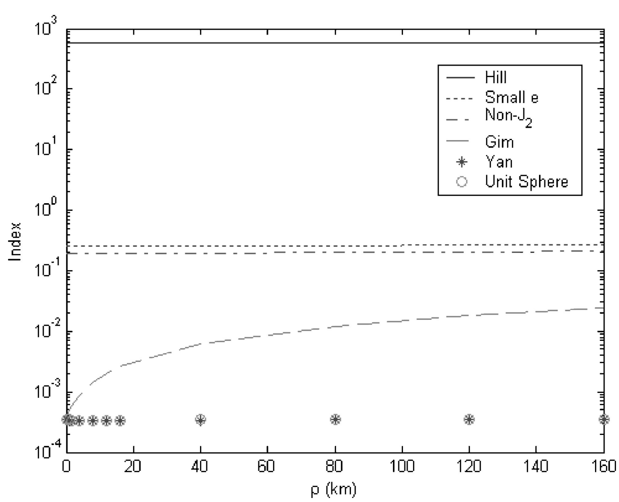

Fig. 5 Index comparison for $e = 0.1$.

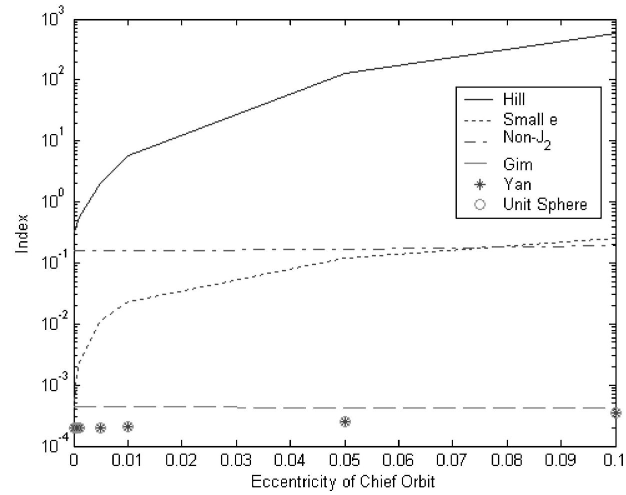

Fig. 6 Index comparison for $\rho = 0.16$ km.

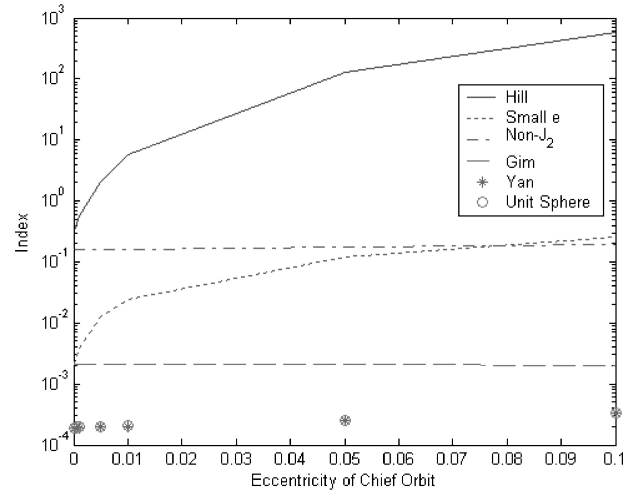

Fig. 7 Index comparison for $\rho = 12$ km.

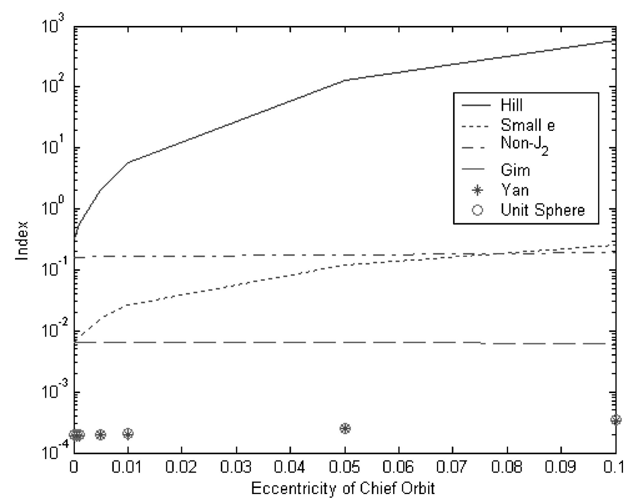

Fig. 8 Index comparison for $\rho = 40$ km.

modeling errors are minimal. For example, because the differential J_2 effects are caused primarily by the inclination difference the effect of not modeling J_2 is very small if the out-of-plane motion is created by only a right-ascension difference. For a specific set of initial conditions, the user would have to compute the index for just those initial conditions.

In Figs. 2–5 the index for Hill's equation and the non-J_2 theory are almost constant. The non-J_2 index is also constant with PCO size as shown in Figs. 6–9. Because the non-J_2 theory has no eccentricity approximation, its index shows the effect of not modeling J_2 for small relative motion orbits. The difference between the non-J_2 theory and the Gim–Alfriend index represents the effect of not modeling J_2; it is significant. Even for $e = 0.001$, there is a factor of four difference between the two indices.

The difference between the Hill index and the non-J_2 index represents the effects of not modeling the eccentricity. Even for $e = 0.001$,

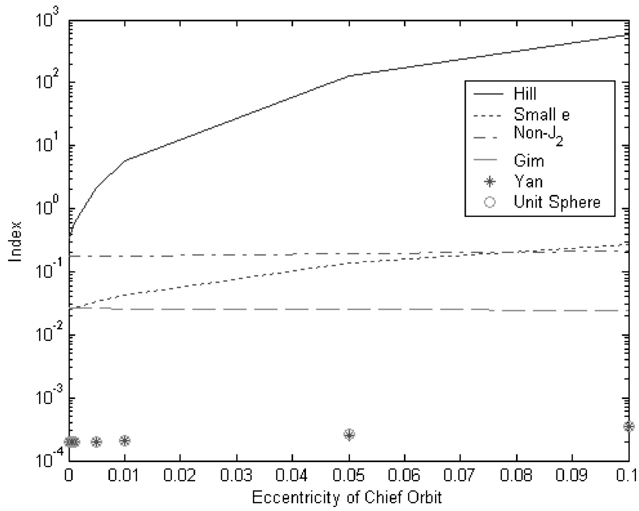

Fig. 9 Index comparison for $\rho = 160$ km.

it is substantial. Figure 6 shows how it grows with increasing eccentricity.

In Fig. 6 the small e index and non-J_2 index are equal at about $e = 0.08$. This is the point where neglecting second-order eccentricity effects is about equal to neglecting the J_2 effects.

For both the Vadali unit sphere and Yan–Alfriend methods, the index is essentially constant for all cases and approximately equal to 10^{-3}. This means they provide an accurate representation of the motion for all eccentricities and relative motion orbits as large as 160 km. As expected, the index for the Gim–Alfriend theory is constant with eccentricity because it has no eccentricity approximation. Its sensitivity to the orbit size is evident, but even for PCOs as large as 40 km it is still less than 0.01.

In comparing the small e and the Gim–Alfriend indices, one can see the difference even for $e = 0.001$, even though the index is small. Figure 6 shows that the difference is two orders of magnitude at $e = 0.01$, meaning the small e theory might not provide sufficient accuracy for $e = 0.01$.

Conclusions

The modeling error index presented in this paper is an effective tool for evaluating the accuracy of approximate approaches of modeling relative motion and should aid designers in determining what effects need to be included in the reference orbit model. The numerical results show that, in general, neglecting J_2 effects is significant, even though there are initial conditions for which the differential J_2 effects will be minimal. In addition, neglecting eccentricity effects, even for $e < 0.001$, can be significant. For $e < 0.01$ the small e theory, which includes the first-order eccentricity effects for the non-J_2 terms and zeroth-order eccentricity effects for the J_2 terms, provides reasonable results. For the theories evaluated, the sequence of the index from high to low, with low being the most accurate, for the cases evaluated is Hill's equations, non-J_2, small eccentricity, Gim–Alfriend index. The unit sphere method and the Yan–Alfriend nonlinear method indices are the lowest and essentially equal. The unit sphere approach and Yan–Alfriend nonlinear theory are accurate for all eccentricities and relative motion orbits as large as 160 km in low Earth orbit. The results presented in this paper should be valid for any relative motion orbit with out-of-plane motion, such as the circular relative motion orbit, when there is a differential inclination. Because the differential J_2 effects are primarily caused by a differential inclination, the results presented here on the effects of J_2 do not apply for in-plane relative motion orbits, or when the out-of-plane motion is caused by only a right-ascension difference.

Appendix: Small-Eccentricity State Transition Matrix

In this Appendix the relative motion state transition matrix (STM) for small eccentric chief orbits is derived. This STM will include $\mathcal{O}(e)$ terms for the non-J_2 portion and only $\mathcal{O}(e^0)$ for the J_2 portion. The STM is obtained from[8] by setting $q_1 = q_2 = 0$ in all the terms multiplied by J_2 and retaining only the first-order terms in q_1 and q_2 in the non-J_2 terms. The notation of Ref. 8 will be used. Assume $\Sigma = A(t) + \alpha B(t)$, R is radius of the chief orbit, p is a semiparameter, and V_r and V_t are the radial and transversal velocity of the chief, respectively.

Σ Matrix (Refer to Appendix A of Ref. 8)

The matrices Σ and Σ^{-1} as they are. $\mathcal{O}(e)$ approximations for R, V_r, V_t, and p could be made, but this does not shorten the calculations so they are not changed.

Mean to Osculating (Refer to Appendix E of Ref. 8)

Because no eccentricity terms are retained, the mean to osculating transformation for zero eccentricity is

$$\boldsymbol{e}_{\text{osc}} = \boldsymbol{e}_m + \varepsilon\left[\boldsymbol{e}^{(lp)} + \boldsymbol{e}^{(sp1)} + \boldsymbol{e}^{(sp2)}\right]$$

$$\boldsymbol{e} = (a, \theta, i, q_1, q_2, \Omega)^T$$

$$\bar{a} = a/R_e, \qquad \theta = f + \omega, \quad q_1 = e\cos\omega, \qquad q_2 = e\sin\omega \tag{A1}$$

$$\varepsilon = -J_2, \qquad \boldsymbol{e}^{(lp)} = 0 \tag{A2}$$

$$a^{(sp1)} = \theta^{(sp1)} = i^{(sp1)} = \Omega^{(sp1)} = 0$$

$$q_1^{(sp1)} = \frac{3(1 - 3\cos^2 i)}{4\bar{a}^2}\cos\theta, \qquad q_2^{(sp1)} = \frac{3(1 - 3\cos^2 i)}{4\bar{a}^2}\sin\theta \tag{A3}$$

$$a^{(sp2)} = -\left(\frac{3R_e\sin^2 i}{2\bar{a}}\right)\cos 2\theta$$

$$\lambda^{(sp2)} = -\frac{3(3 - 5\cos^2 i)}{8\bar{a}^2}\sin 2\theta$$

$$\theta^{(sp2)} = \lambda^{(sp2)} + \left(\frac{\sin^2 i}{\bar{a}^2}\right)\sin 2\theta, \qquad i^{(sp2)} = -\left(\frac{3\sin 2i}{8\bar{a}^2}\right)\cos 2\theta$$

$$q_1^{(sp2)} = -\left(\frac{\sin^2 i}{8\bar{a}^2}\right)(3\cos\theta + 7\cos 3\theta)$$

$$q_2^{(sp2)} = \left(\frac{\sin^2 i}{8\bar{a}^2}\right)(3\sin\theta - 7\sin 3\theta)$$

$$\Omega^{(sp2)} = -\left(\frac{3\cos i}{4\bar{a}^2}\right)\sin 2\theta \tag{A4}$$

D Matrix (Refer to Appendix E of Ref. 8)

Only the nonzero terms are presented. Let $\Theta = 1/(1 - 5\cos^2 i)$:

$$D = \frac{\partial\boldsymbol{e}_{\text{osc}}}{\partial\boldsymbol{e}_m} = 1 - J_2\left[D^{(lp)} + D^{(sp1)} + D^{(sp2)}\right] \tag{A5}$$

$$D_{24}^{(lp)} = -\frac{\sin^2 i}{8\bar{a}^2}(1 - 10\Theta\cos^2 i)\sin\theta$$

$$D_{25}^{(lp)} = -\frac{\sin^2 i}{8\bar{a}^2}(1 - 10\Theta\cos^2 i)\cos\theta \tag{A6a}$$

$$D_{44}^{(lp)} = -\frac{\sin^2 i}{16\bar{a}^2}(1 - 10\Theta\cos^2 i), \qquad \Theta = (1 - 5\cos^2 i)^{-1} \tag{A6b}$$

$$D_{55}^{(lp)} = \frac{\sin^2 i}{16\bar{a}^2}(1 - 10\Theta\cos^2 i) \tag{A6c}$$

$$D_{14}^{(sp1)} = \frac{3R_e(1-3\cos^2 i)}{2\bar{a}}\cos\theta$$

$$D_{15}^{(sp1)} = \frac{3R_e(1-3\cos^2 i)}{2\bar{a}}\sin\theta \tag{A7a}$$

$$D_{24}^{(sp1)} = \frac{9}{4\bar{a}^2}(1-5\cos^2 i)\sin\theta$$

$$D_{25}^{(sp1)} = -\frac{9}{4\bar{a}^2}(1-5\cos^2 i)\cos\theta \tag{A7b}$$

$$D_{41}^{(sp1)} = -\frac{3(1-3\cos^2 i)}{2R_e\bar{a}^3}\cos\theta, \qquad D_{42}^{(sp1)} = -\frac{3(1-3\cos^2 i)}{4\bar{a}^2}\sin\theta$$

$$D_{43}^{(sp1)} = \frac{9\sin 2i}{4\bar{a}^2}\cos\theta \tag{A7c}$$

$$D_{44}^{(sp1)} = \frac{3(1-3\cos^2 i)}{8\bar{a}^2}(2+\cos 2\theta)$$

$$D_{45}^{(sp1)} = \frac{3(1-3\cos^2 i)}{8\bar{a}^2}\sin 2\theta \tag{A7d}$$

$$D_{51}^{(sp1)} = -\frac{3(1-3\cos^2 i)}{2R_e\bar{a}^3}\sin\theta, \qquad D_{52}^{(sp1)} = \frac{3(1-3\cos^2 i)}{4\bar{a}^2}\cos\theta$$

$$D_{53}^{(sp1)} = \frac{9\sin 2i}{4\bar{a}^2}\cos\theta \tag{A7e}$$

$$D_{54}^{(sp1)} = \frac{3(1-3\cos^2 i)}{8\bar{a}^2}\sin 2\theta$$

$$D_{55}^{(sp1)} = \frac{3(1-3\cos^2 i)}{8\bar{a}^2}(2-\cos 2\theta) \tag{A7f}$$

$$D_{64}^{(sp1)} = \frac{9\cos i}{2\bar{a}^2}\sin\theta, \qquad D_{65}^{(sp1)} = -\frac{9\cos i}{2\bar{a}^2}\cos\theta \tag{A7g}$$

$$D_{11}^{(sp2)} = \left(\frac{3\sin^2 i}{2\bar{a}^2}\right)\cos 2\theta, \qquad D_{12}^{(sp2)} = \left(\frac{3R_e\sin^2 i}{\bar{a}}\right)\sin 2\theta$$

$$D_{13}^{(sp2)} = -\left(\frac{3R_e\sin 2i}{2\bar{a}}\right)\cos 2\theta \tag{A8a}$$

$$D_{14}^{(sp2)} = -\left(\frac{9R_e\sin^2 i}{4\bar{a}}\right)(\cos\theta+\cos 3\theta)$$

$$D_{15}^{(sp2)} = \left(\frac{9R_e\sin^2 i}{4\bar{a}}\right)(\sin\theta-\sin 3\theta) \tag{A8b}$$

$$D_{21}^{(sp2)} = -\left(\frac{6-7\sin^2 i}{4R_e\bar{a}^3}\right)\sin 2\theta$$

$$D_{22}^{(sp2)} = \left(\frac{6-7\sin^2 i}{4\bar{a}^2}\right)\cos 2\theta$$

$$D_{23}^{(sp2)} = -\left(\frac{7\sin 2i}{8\bar{a}^2}\right)\sin 2\theta \tag{A8c}$$

$$D_{24}^{(sp2)} = \left(\frac{24-47\sin^2 i}{32\bar{a}^2}\right)\sin\theta + \frac{\cos^2 i}{4\bar{a}^2}\sin 3\theta$$

$$D_{25}^{(sp2)} = \left(\frac{24-47\sin^2 i}{32\bar{a}^2}\right)\cos\theta - \frac{\cos^2 i}{4\bar{a}^2}\cos 3\theta \tag{A8d}$$

$$D_{31}^{(sp2)} = \left(\frac{3\sin 2i}{4R_e\bar{a}^3}\right)\cos 2\theta, \qquad D_{32}^{(sp2)} = \left(\frac{3\sin 2i}{4\bar{a}^2}\right)\sin 2\theta$$

$$D_{33}^{(sp2)} = -\left(\frac{3\cos 2i}{4\bar{a}^2}\right)\cos 2\theta \tag{A8e}$$

$$D_{34}^{(sp2)} = -\left(\frac{\sin 2i}{8\bar{a}^2}\right)(3\cos\theta+\cos 3\theta)$$

$$D_{35}^{(sp2)} = \left(\frac{\sin 2i}{8\bar{a}^2}\right)(3\sin\theta-\sin 3\theta) \tag{A8f}$$

$$D_{41}^{(sp2)} = \left(\frac{\sin^2 i}{4R_e\bar{a}^3}\right)(3\cos\theta+7\cos 3\theta)$$

$$D_{42}^{(sp2)} = \left(\frac{3\sin^2 i}{8\bar{a}^2}\right)(\sin\theta+7\sin 3\theta) \tag{A8g}$$

$$D_{43}^{(sp2)} = -\left(\frac{\sin 2i}{8\bar{a}^2}\right)(3\cos\theta+7\cos 3\theta) \tag{A8h}$$

$$D_{44}^{(sp2)} = -\left(\frac{3\sin^2 i}{16\bar{a}^2}\right)(3+10\cos 2\theta+3\cos 4\theta)$$

$$D_{45}^{(sp2)} = \frac{3(3-5\cos^2 i)}{8\bar{a}^2}\sin 2\theta - \left(\frac{9\sin^2 i}{16\bar{a}^2}\right)\sin 4\theta \tag{A8i}$$

$$D_{51}^{(sp2)} = -\left(\frac{\sin^2 i}{4R_e\bar{a}^3}\right)(3\sin\theta-7\sin 3\theta)$$

$$D_{52}^{(sp2)} = \left(\frac{3\sin^2 i}{8\bar{a}^2}\right)(\cos\theta-7\cos 3\theta) \tag{A8j}$$

$$D_{53}^{(sp2)} = \left(\frac{\sin 2i}{8\bar{a}^2}\right)(3\sin\theta-7\sin 3\theta) \tag{A8k}$$

$$D_{54}^{(sp2)} = -\frac{3(3-5\cos^2 i)}{8\bar{a}^2}\sin 2\theta - \left(\frac{9\sin^2 i}{16\bar{a}^2}\right)\sin 4\theta$$

$$D_{55}^{(sp2)} = \left(\frac{3\sin^2 i}{16\bar{a}^2}\right)(3-10\cos 2\theta+3\cos 4\theta) \tag{A8l}$$

$$D_{61}^{(sp2)} = \left(\frac{3\cos i}{2R_e\bar{a}^3}\right)\sin 2\theta, \qquad D_{62}^{(sp2)} = -\left(\frac{3\cos i}{2\bar{a}^2}\right)\cos 2\theta$$

$$D_{63}^{(sp2)} = \left(\frac{3\sin i}{4\bar{a}^2}\right)\sin 2\theta \tag{A8m}$$

$$D_{64}^{(sp2)} = -\left(\frac{\cos i}{4\bar{a}^2}\right)(3\sin\theta+\sin 3\theta)$$

$$D_{65}^{(sp2)} = -\left(\frac{\cos i}{4\bar{a}^2}\right)(3\cos\theta-\cos 3\theta) \tag{A8n}$$

$\bar{\phi}_{\bar{e}}$ Matrix (Refer to Appendix D of Ref. 8)

Again, only the nonzero terms are supplied:

$$\alpha = 3J_2R_e^2, \qquad G_\theta = \frac{nR}{V_t}, \qquad G_{\theta_0} = -G_\theta(t=t_0)$$

$$G_{q_1} = -\left(\frac{R}{a}\right)\left(1+\frac{R}{a}\right)\sin\theta, \qquad G_{q_{10}} = -G_{q_1}(t=t_0)$$

$$G_{q_2} = \left(\frac{R}{a}\right)\left(1+\frac{R}{a}\right)\cos\theta, \qquad G_{q_{20}} = -G_{q_2}(t=t_0) \tag{A9}$$

$$\bar{\phi}_{\bar{e}11} = 1 \tag{A10}$$

$$\bar{\phi}_{\bar{e}21} = -\frac{3n_0(t-t_0)}{2a_0 G_\theta}\left[1 + \left(\frac{7\alpha}{6a_0^2}\right)\left(4\cos^2 i_0 - 1\right)\right]$$

$$\bar{\phi}_{\bar{e}22} = -\frac{G_{\theta_0}}{G_\theta} \tag{A11a}$$

$$\bar{\phi}_{\bar{e}23} = -\frac{2\alpha n_0(t-t_0)\sin 2i_0}{a_0^2 G_\theta} \tag{A11b}$$

$$\bar{\phi}_{\bar{e}24} = -\frac{1}{G_\theta}\left[G_{q_{10}} + G_{q_1}\cos(\Delta\omega) + G_{q_2}\sin(\Delta\omega)\right]$$

$$\Delta\omega = \dot{\omega}^{(s)}(t-t_0) \tag{A11c}$$

$$\bar{\phi}_{\bar{e}25} = -\frac{1}{G_\theta}\left[G_{q_{20}} - G_{q_1}\sin(\Delta\omega) + G_{q_2}\cos(\Delta\omega)\right] \tag{A11d}$$

$$\bar{\phi}_{\bar{e}33} = 1 \tag{A12}$$

$$\bar{\phi}_{\bar{e}44} = \cos(\Delta\omega), \qquad \bar{\phi}_{\bar{e}45} = -\sin(\Delta\omega) \tag{A13a}$$

$$\bar{\phi}_{\bar{e}54} = \sin(\Delta\omega), \qquad \bar{\phi}_{\bar{e}55} = \cos(\Delta\omega) \tag{A13b}$$

$$\bar{\phi}_{\bar{e}61} = \left(\frac{7\alpha}{4a_0^2}\right)\left(\frac{n_0\cos i_0}{a_0}\right)(t-t_0)$$

$$\bar{\phi}_{\bar{e}63} = \left(\frac{\alpha}{2a_0^2}\right)(n_0\sin i_0)(t-t_0), \qquad \bar{\phi}_{\bar{e}66} = 1 \tag{A13c}$$

Acknowledgment

This research was supported by NASA Goddard Space Flight Center under Grant NAG5-11349. We thank them for their support.

References

[1]Clohessy, W. H., and Wiltshire, R. S., "Terminal Guidance System for Satellite Rendezvous," *Journal of the Astronautical Sciences*, Vol. 27, No. 9, 1960, pp. 653–678.

[2]Hill, G. W., "Researches in the Lunar Theory," *American Journal of Mathematics*, Vol. 1, 1878, pp. 5–26.

[3]Lawden, D. F., *Optimal Trajectories for Space Navigation*, Butterworths, London, 1963, pp. 79–86.

[4]Tschauner, J., and Hempel, P., "Optimale Beschleunigeungsprogramme fur das Rendezvous-Manover," *Astronautica Acta*, Vol. 10, 1964, pp. 296–307.

[5]Anthony, M. L., and Sasaki, F. T., "Rendezvous Problem for Nearly Circular Orbits," *AIAA Journal*, Vol. 3, No. 9, 1965, pp. 1666–1673.

[6]London, H. S., "Second Approximation to the Solution of the Rendezvous Equations," *AIAA Journal*, Vol. 1, No. 7, 1963, pp. 1691–1693.

[7]Carter, T. E., "New Form for the Optimal Rendezvous Equations near a Keplerian Orbit," *Journal of Guidance, Control, and Dynamics*, Vol. 13, No. 1, 1990, pp. 183–186.

[8]Gim, D.-W., and Alfriend, K. T., "State Transition Matrix of Relative Motion for the Perturbed Noncircular Reference Orbit," *Journal of Guidance, Control, and Dynamics*, Vol. 26, No. 6, 2003, pp. 956–971.

[9]Inalhan, G., and How, J., "Relative Dynamics and Control of Spacecraft Formations in Elliptic Orbits," *Journal of Guidance, Control, and Dynamics*, Vol. 25, No. 1, 2002, pp. 48–59.

[10]Karlgard, C. D., and Lutze, F. H., "Second Order Relative Motion Equations," *Advances in the Astronautical Sciences*, Vol. 109, Pt. 3, 2002, pp. 2429–2448.

[11]Mitchell, J. W., and Richardson, D. L., "A Third Order Analytical Solution for Relative Motion with a Circular Reference Orbit," *Journal of the Astronautical Sciences*, Vol. 51, No. 1, 2003, pp. 1–12.

[12]Vaddi, S. S., Vadali, S. R., and Alfriend, K. T., "Formation Flying: Accommodating Nonlinearity and Eccentricity Perturbations," *Journal of Guidance, Control, and Dynamics*, Vol. 26, No. 2, 2002, pp. 214–223.

[13]Alfriend, K. T., Yan, H., and Vadali, S. R., "Nonlinear Considerations in Satellite Formation Flying," AIAA Paper 2002-4741, Aug. 2002.

[14]Alfriend, K. T., and Yan, H., "An Orbital Elements Approach to the Nonlinear Formation Flying Problem," International Formation Flying Conf.: Missions and Technologies, Toulouse, France, Oct. 2002.

[15]Junkins, J. L., Akella, M. R., and Alfriend, K. T., "Non-Gaussian Error Propagation in Orbital Mechanics," *Journal of the Astronautical Sciences*, Vol. 44, Oct.–Dec. 1996, pp. 541–563.

[16]Junkins, J. L., "How Nonlinear Is It?" *Advances in the Astronautical Sciences*, Vol. 115, 2003, pp. 3–52.

[17]Vadali, S. R., "An Analytical Solution for Relative Motion of Satellites," Conf. on Dynamics and Control of Space Systems, Cranfield Univ., Cranfield, England, U.K., July 2002.

[18]Sengupta, P., Vadali, S. R., and Alfriend, K. T., "Modeling and Control of Satellite Formations in High Eccentricity Orbits," *Advances in the Astronautical Sciences*, Vol. 115, 2003, pp. 325–350.

[19]Vadali, S. R., Vaddi, S. S., and Alfriend, K. T., "A New Concept for Controlling Formation Flying Satellite Constellations," *Advances in the Astronautical Sciences*, Vol. 108, 2001, pp. 1631–1648.

[20]Brouwer, D., "Solution of the Problem of Artificial Satellite Theory Without Drag," *Astronomical Journal*, Vol. 64, No. 1274, 1959, pp. 378–397.

[21]Yan, H., Sengupta, P., Vadali, S. R., and Alfriend, K. T., "Development of a State Transition Matrix for Relative Motion Using the Unit Sphere Approach," American Astronautical Society, AAS Paper 04-163, Feb. 2004.

[22]Vallado, D. A., *Fundamentals of Astrodynamics and Applications*, McGraw–Hill, New York, 1997, pp. 343–368.

[23]Schaub, H., and Alfriend, K. T., "J_2 Invariant Orbits for Spacecraft Formations," *Celestial Mechanics and Dynamical Astronomy*, Vol. 79, 2001, pp. 77–95.